Redox Biochemistry and Chemistry 8 (2024) 100021

Contents lists available at ScienceDirect

Redox Biochemistry and Chemistry

journal homepage: www.journals.elsevier.com/redox-biochemistry-and-chemistry

Lactoperoxidase catalytically oxidize hydrogen sulfide via intermediate formation of sulfheme derivatives

Bessie B. Ríos-González [a,1], Andrea Domán [b,1], Tamás Ditrói [b], Dorottya Garai [b], Leishka D. Crespo [a], Gary J. Gerfen [c], Paul G. Furtmüller [d], Péter Nagy [b,e,f,*], Juan López-Garriga [a,**]

[a] Department of Chemistry, University of Puerto Rico, Mayagüez Campus, P.O. Box 9019, Mayagüez, 00681-9019, Puerto Rico
[b] Department of Molecular Immunology and Toxicology and the National Tumor Biology Laboratory, National Institute of Oncology, Ráth György street 7-9, Budapest, 1122, Hungary
[c] Department of Physiology & Biophysics, Albert Einstein College of Medicine, 1300 Morris Park Ave, Bronx, NY, 10461, United States
[d] Institute of Biochemistry, Department of Chemistry, University of Natural Resources and Life Sciences, Vienna, Muthgasse 18, Vienna, Austria, A-1190
[e] Department of Anatomy and Histology, ELKH Laboratory of Redox Biology, University of Veterinary Medicine, István street 2, Budapest, 1078, Hungary
[f] Chemistry Institute, University of Debrecen, Egyetem square 1, Debrecen, 4032, Hungary

ARTICLE INFO

Keywords:
Lactoperoxidase
Hydrogen sulfide
Sulfheme protein
LPO turnover
Sulfate
Inorganic polysulfide species

ABSTRACT

The biological chemistry of hydrogen sulfide (H_2S) with physiologically important heme proteins is in the focus of redox biology research. In this study, we investigated the interactions of lactoperoxidase (LPO) with H_2S in the presence and absence of molecular dioxygen (O_2) or hydrogen peroxide (H_2O_2). Under anaerobic conditions, native LPO forms no heme-H_2S complex upon sulfide exposure. However, under aerobic conditions or in the presence of H_2O_2 the formation of both ferrous and ferric sulfheme (sulfLPO) derivatives was observed based on the appearances of their characteristic optical absorptions at 638 nm and 727 nm, respectively. Interestingly, we demonstrate that LPO can catalytically oxidize H_2S by H_2O_2 via intermediate formation of relatively short-lived ferrous and ferric sulfLPO derivatives. Pilot product analyses suggested that the turnover process generates oxidized sulfide species, which include sulfate (SO_4^{2-}) and inorganic polysulfides (HS_x^-; x = 2–5). These results indicated that H_2S can serve as a non-classical LPO substrate by inducing a reversible sulfheme-like modification of the heme porphyrin ring during turnover. Furthermore, electron paramagnetic resonance data suggest that H_2S can act as a scavenger of H_2O_2 in the presence of LPO without detectable formation of any carbon-centered protein radical species, suggesting that H_2S might be capable of protecting the enzyme from radical-mediated damage. We propose possible mechanisms, which explain our results as well as contrasting observations with other heme proteins, where either no sulfheme formation was observed or the generation of sulfheme derivatives provided a dead end for enzyme functions.

1. Introduction

It is now widely accepted that under controlled physiological conditions endogenous H_2S [1–3] and/or derived reactive sulfur species are involved in cellular signaling [4–10]. An emerging number of studies show that interactions of heme proteins with hydrogen sulfide are both physiologically and pathologically determining factors of hydrogen sulfide biochemistry [11–18].

Lactoperoxidase (LPO) together with myeloperoxidase (MPO), eosinophil peroxidase (EPO) and thyroid peroxidase (TPO) are members of mammalian heme peroxidases and their primary function is to produce antimicrobial oxidants to protect the host from invading pathogens [19–21]. Lactoperoxidase is found in mammary, salivary, lachrymal and bronchial submucosal glands. It is responsible for non-specific humoral

* Corresponding author. Department of Molecular Immunology and Toxicology and the National Tumor Biology Laboratory, National Institute of Oncology, Ráth György street 7-9, Budapest, 1122, Hungary.
** Corresponding author.
E-mail addresses: peter.nagy@oncol.hu (P. Nagy), juan.lopez16@upr.edu (J. López-Garriga).
[1] Equal 1st author.

https://doi.org/10.1016/j.rbc.2024.100021
Received 17 November 2023; Received in revised form 7 March 2024; Accepted 3 April 2024
Available online 4 April 2024

immune response against respiratory viruses, fungi and bacteria within mucous membranes by producing antimicrobial substances, primarily hypothiocyanite ($OSCN^-$). Furthermore, it participates in the protection against oxidative stress, hindering the formation of more destructive reactive oxygen species (ROS) as a hydrogen peroxide scavenger. Thus, LPO is an important element of the airway host defense system [22–24].

Structurally, the heme prosthetic group in LPO is attached to the protein through ester bonds of Asp225 and Glu375 to the porphyrin (Por) motif and coordination of the heme iron to His468 at the proximal position (Fig. 1A) [20]. In its resting form, the heme group of LPO exists in a six-coordinate high-spin aqua ferric state, coordinating a water molecule in the distal position of the heme group [25]. Regarding its biologically relevant activities, two main catalytic cycles of peroxidases are distinguished. In the halogenation cycle, LPO uses H_2O_2 to primarily catalyze the oxidation of inorganic thiocyanate (SCN^-) to form hypothiocyanite ($OSCN^-$) in a two-electron oxidation process (Fig. 1B) [26]. Alternatively, H_2O_2-mediated oxidation of organic substrates such as phenols or aromatic amines can be catalyzed by LPO in two consecutive one-electron redox reactions, which represents the so-called peroxidase cycle (Fig. 1B) [27–29]. Both catalytic cycles involve the intermediate formation of Compound 0 (Cpd 0: Por-Fe(III)–OOH) as well as the oxo-ferryl enzyme forms Compound I (containing an oxoiron (IV) heme and a porphyrin π-cation radical; Cpd I: $^{+\bullet}$Por-Fe(IV)═O) or Compound II (containing an oxoiron(IV) heme; Cpd II: Por-Fe(IV)═O). It was suggested, that in the absence of substrate, Compound I may be able to spontaneously decay to a more stable amino acid radical ($^{\bullet}$aa) containing species, designated as Compound I* (containing an oxoiron (IV) heme and an amino acid radical; Cpd I*: $^{+\bullet}$aa–Por-Fe(IV)═O) [30]. Furthermore, Compound 0 may also be generated through the consecutive generation of ferrous LPO and Compound III (Cpd III: Por-Fe(II)–O_2 ↔ Por-Fe(III)–$O_2^{\bullet-}$) as shown in Fig. 1D [31].

Hydrogen sulfide can favourably coordinate to the available coordination site of heme metal centers and reduce the iron ion in a subsequent reaction [15,16]. It can also modify the prosthetic group via sulfur incorporation into one of the pyrrole rings of the porphyrin frame at β-pyrrole positions, resulting in the formation of sulfheme species [12,33]. Several (but not all) heme proteins form the corresponding sulfheme derivative including hemoglobin (Hb) [34–36], myoglobin (Mb) [35–39] or catalase (CAT) [39,40] and based on UV–vis spectroscopic data this reaction was also proposed for LPO [41]. On mechanistic grounds, Compound II was identified as a central intermediate in sulfheme formation and the $HS^{\bullet}$ radical as the attacking agent [12]. It was also suggested that the histidine residue in the distal position of the heme pocket is an essential [12,35,42], but not a sufficient [16,17] requirement for sulfheme generation.

Sulfheme derivatives may exhibit altered protein functions. For example, the oxygen binding affinities of sulfhemoglobin and sulfmyoglobin are significantly reduced compared to functional Hb and Mb, respectively [37,43]. In addition, their formation is irreversible under physiological conditions. Sulfcatalse does not possess any catalase activity, however, it is less stable and catalase can be regenerated by its reaction with oxygen [39,40]. Sulfheme lactoperoxidase (sulfLPO) formation was investigated by Nakamura and coworkers [41]. They proposed that the reaction of LPO Compound II with hydrogen sulfide gives ferric and ferrous sulfLPO. Activity measurements suggested, that LPO loses its activity upon sulfLPO formation, but in the presence of excess sulfide, it may be recovered over time [41]. However, further experiments are in order to corroborate these results and for a deeper understanding of sulfLPO formation and its potential physiological relevance. In addition, the catalytic turnover of LPO using sulfide as a substrate has not been functionally investigated and no product analyses for these enzymatic reactions were reported.

We previously conducted comprehensive kinetic analyses for the reactions of MPO with H_2S [16,17], and the current study is aimed at providing insights into the catalytic oxidation of sulfide by LPO. Here we show that: (1) depending on the applied oxidizing agent and experimental conditions, LPO catalyzed the oxidation of sulfide via intermediate formation of ferrous sulfLPO and/or ferric sulfLPO; (2) turnover of sulfLPO derivatives did not regenerate sulfide, but instead lead to oxidized sulfur derivatives including SO_4^{2-} and inorganic hydropolysulfides; (3) electron paramagnetic resonance (EPR) data showed that in the presence of LPO, H_2S can scavenge H_2O_2 without detectable formation of a carbon-centered radical on the LPO peptide chain, suggesting an antioxidant property for hydrogen sulfide in these redox events.

2. Materials and methods

All the reagents and proteins were purchased from Sigma-Aldrich unless otherwise indicated. LPO from bovine milk (Sigma type L-

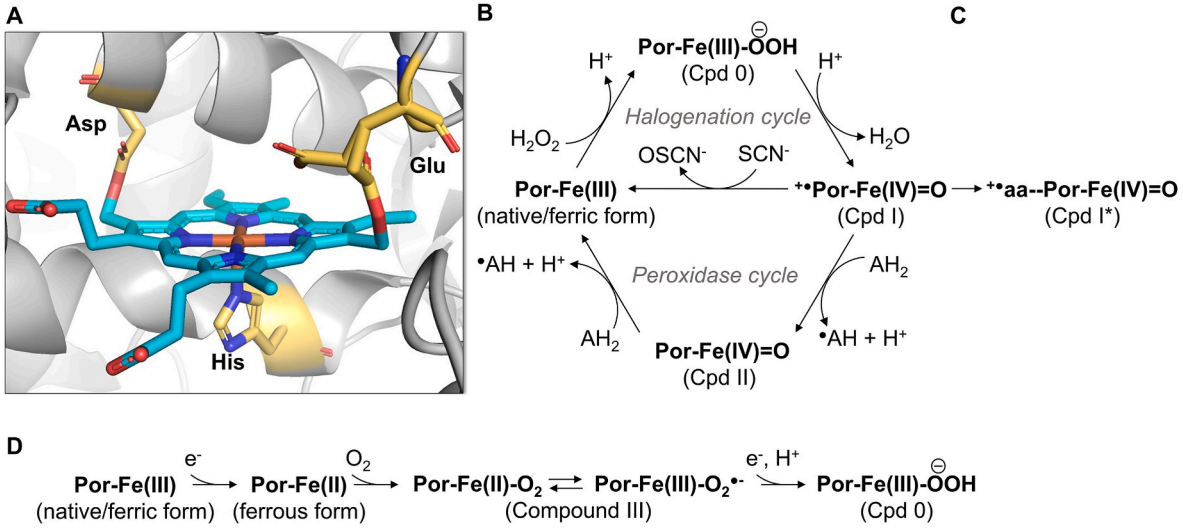

Fig. 1. Structural properties and catalytic turnover of lactoperoxidase. A) Active site structure of LPO (PDB: 5b72) [32]; cyan blue: carbon in porphyrin (Por); yellow: carbon in heme binding protein residues (His: proximal histidine, Glu: glutamic acid, Asp: aspartic acid); orange: iron ion; red: oxygen; dark blue: nitrogen. B) Halogenation cycle and peroxidase cycle through Compound 0, where AH_2 is a reducing substrate. C) Compound I* formation. D) Previously proposed acid-catalyzed formation of Compound 0 through Compound III [31]. (For interpretation of the references to color in this figure legend, the reader is referred to the Web version of this article.)

2005) was purchased as a lyophilized powder. The concentration of LPO-Fe(III) was determined using the extinction coefficient $\varepsilon_{412} = 114\ mM^{-1}\ cm^{-1}$ [44]. H_2O_2 was obtained as a 30% solution. The working solutions were prepared using a 0.1 M KH_2PO_4/Na_2HPO_4 buffer (pH 7.0) containing 1 mM ethylenediaminetetraacetic acid (EDTA). H_2S stock solutions were prepared daily from Na_2S x $9H_2O$ in tightly sealed amber glass bottles. These solutions were diluted in KH_2PO_4/Na_2HPO_4 containing buffers. Important to note, that in solutions, H_2S is in equilibrium with its deprotonated forms: $H_2S \leftrightarrow HS^- + H^+ \leftrightarrow S_2^- + 2\ H^+$. At neutral pH HS^- is the dominating species [45] but for simplicity, sulfide solution will be referred as H_2S solution in the text. All other chemicals were ACS reagent grade or better.

2.1. UV–vis measurements for the reactions of LPO with H_2S in the presence and absence of O_2 and H_2O_2

The interactions of H_2S with LPO were measured with an Agilent 8453 spectrophotometer using sealed quartz cuvettes (1 cm path length) with a septum. The reactions were made by titrating 1 μL of the reagents with a gastight syringe into the LPO samples in the cuvette. All the measurements were performed at 25 °C and pH 7.0 in 0.1 M KH_2PO_4/Na_2HPO_4 buffer.

To investigate the interactions of native ferric LPO-Fe(III) with H_2S in the presence of O_2, H_2S solution was added to the LPO sample in the cuvette. The final concentration of the reaction mixture was 3 μM ferric LPO-Fe(III) and 150 μM H_2S.

For the anaerobic experiments the buffer, the Na_2S x 9 H_2O, the sodium dithionite (DT), and the protein solutions were prepared anaerobically by degassing for 30 min and flushing for at least 20 min with nitrogen. In the first experimental setup, 2.7 μM ferric LPO-Fe(III) was reacted with 150 μM H_2S under anaerobic conditions. After about 1 h of incubation, the sample was purged for 1 min with O_2. In the second experimental setup, first, the ferrous LPO-Fe(II) derivative was generated in the reaction of ferric LPO-Fe(III) with DT. To accomplish full reduction of ferric LPO-Fe(III) a sevenfold excess of DT from a freshly prepared anaerobic stock solution was added to 2.7 μM LPO-Fe(III). DT loss was monitored by the absorbance decrease at 315 nm. This was followed by reacting the ferrous LPO with 50 μM H_2S under anaerobic conditions. After a short incubation period with sulfide, the mixture was purged for 1 min with O_2 and the associated spectral changes were recorded.

The experimental turnover of sulfLPO was followed in the reaction of native LPO-Fe(III) with H_2O_2 and H_2S. Initially, 2.1 μM LPO-Fe(III) was reacted with 10.5 μM H_2O_2. After 2 min of incubation, 375 μM H_2S was added to the reaction mixture. The absorption spectra were recorded immediately after H_2S addition and in every 2 min until reaching an equilibrium with the characteristic electronic transition state of the native protein. Then a second aliquot of 21 μM of H_2O_2 was added to the sample leading to a new increase of the 638 nm peak intensity. The process was repeated several times until all H_2S was consumed and the reaction products were only related to these in the classical peroxidase cycle and the 638 nm band was completely absent.

2.2. Stopped-flow measurements of LPO with H_2S under aerobic and anaerobic conditions

The interactions of native LPO and the oxo-ferryl derivative of LPO with H_2S were measured using a π*-180 sequential mixing stopped-flow instrument from Applied Photophysics Inc. (Leatherhead, UK) equipped with a photodiode array detection. The measurements were performed at 25 °C and pH 7.0 in 0.1 M KH_2PO_4/Na_2HPO_4 buffer. The interactions of H_2S with native LPO-Fe(III) were followed under anaerobic conditions. These measurements were made by purging the KH_2PO_4/Na_2HPO_4 buffer (0.1 M), the H_2S, and the protein solutions with nitrogen gas for at least 30 min. Then 12 μM of native LPO and 560 μM H_2S were introduced to the stopped-flow instrument in gas-tight syringes. Reactions were performed in a volume ratio of 1 to 1, so the final concentrations in the reaction mixture were 6 μM LPO-Fe(III) and 280 μM H_2S. The reaction of the LPO oxo-ferryl species was followed in sequential mixing mode. The oxo-ferryl species was prepared by mixing 3.6 μM LPO-Fe(III) with 5 μM hydrogen peroxide in the ageing loop. After a delay of 5 s, 1.8 μM oxo-ferryl species was allowed to react with different concentrations of H_2S (0–600 μM).

2.3. EPR spectroscopy measurements

To get deeper insights into the nature of the LPO intermediate species during enzyme turnover in the presence of H_2O_2 and H_2S, electron paramagnetic resonance (EPR) measurements were carried out by a Varian E−112 spectrometer equipped with a TE_{102} cavity operating at X-band (9 GHz) frequencies. The sample temperature was held at 77 K using an immersion finger dewar. EPR spectra were recorded using 1 mW microwave power, a modulation amplitude of 1.00 × 10.00 G, 0.5 s time constant and 2000 points. The samples were prepared at a pH of 7 in 0.1 M KH_2PO_4/Na_2HPO_4 buffer. For the EPR measurements four reaction mixtures were prepared: 1) 300 μM ferric LPO-Fe(III); 2) 300 μM ferric LPO-Fe(III) with 900 μM H_2O_2; 3) 300 μM ferric LPO-Fe(III) with 900 μM H_2O_2 and 300 μM H_2S and 4) 300 μM ferric LPO-Fe(III) with 900 μM H_2O_2 and 15000 μM H_2S. The different reaction mixtures were prepared in sealed glass bottles from which 200 μL were immediately transferred into quartz EPR tubes (4 mm OD) and frozen in liquid nitrogen. Previously to adding the solutions to the EPR tubes, they were degassed with N_2.

2.4. Measurements of sulfate, sulfane sulfur and inorganic polysulfides production, upon LPO turnover in the presence of H_2O_2 and H_2S

Sulfate production was investigated using 5 μM LPO, which was reacted with 25 μM or 50 μM H_2O_2 and 600 μM, 800 μM or 1000 μM H_2S. The reaction was performed under similar conditions as described in section 2.1, except here, after 3.5 h of LPO turnover in the presence of H_2O_2 and H_2S, the samples were centrifuged for 30 min in a 10 kDa concentrator. The filtrate was recovered to measure sulfate production in the reaction following the procedure established in the literature [46]. Briefly: A 900 μL aliquot was acidified with a conditioning reagent (450 μL) containing concentrated HCl. Barium sulfate was obtained as a precipitate upon adding barium chloride to the solution. Then 1 mL of the solution was transferred to a quartz cuvette to measure the optical density at 420 nm. The concentration of sulfate was determined using a calibration curve previously made in the concentration range of 100 μM–850 μM of sulfate with a 10.4 mM sodium sulfate stock (see e.g. Supplemental Fig. S1).

Formation of sulfane sulfur species during LPO turnover in the presence of H_2O_2 and H_2S was measured with a fluorescence sulfane sulfur-specific probe [47]. Hydrogen sulfide stock solutions were prepared as described previously [2]. A 10 mM stock solution of the sulfane sulfur-specific fluorescent dye, 3′,6′-Di(O-thiosalicyl) fluorescein (Sulfane Sulfur Probe 4 or SSP4, Dojindo), was prepared in dimethyl sulfoxide. SSP4 was used at a final concentration of 500 μM. The production of sulfane sulfur species by LPO in the presence of sulfide and H_2O_2 was determined by spectrofluorimetry in flat bottom, black plates using an Optima Star fluorescent plate reader at emission and excitation wavelengths of 485 nm and 515 nm, respectively [17]. The fluorescence intensity values of the samples were measured every 30 s for 90 min. Sulfane sulfur production was measured with 0.5 μM LPO, 5000 μM sulfide and different concentrations of H_2O_2 (10–100 μM) 30 min after the reactions were initiated by the addition of H_2O_2. Sulfide oxidation in the absence of LPO was also determined under similar conditions in order to subtract non-LPO catalyzed sulfane sulfur production from the kinetic curves.

We used LC/MS-MS to check whether a proportion of the produced sulfane sulfur species represents inorganic polysulfides [48]. Five

reaction mixtures were prepared, each were 300 μL in 100 mM phosphate buffer with 200 μM diethylenetriaminepentaacetic acid (DTPA). LPO, H_2O_2 and H_2S concentrations for the mixtures are shown in Table 1. Samples were incubated for 30 min at 37 °C, then the products were derivatized by adding 30 μL 100 mM β-(4-hydroxyphenyl) ethyl iodoacetamide (HPE-IAM). After 15 min of incubation at 37 °C alkylation reactions were stopped by adding 5 μL 50 % trichloroacetic acid to the samples under vigorous vortexing conditions. Samples were centrifuged (30,000 g, 5 min) and the supernatants were stored in the autosampler at the HPLC in dark vials at 5 °C. A Thermo Ultimate 3000 HLPC system coupled to a Thermo LTQ-XL mass spectrometer was used with a Kinetex C18 column (50 × 2.1 mm, 2.6 μm, Phenomenex) for the separation of the analytes. 50 μL of the derivatized samples were injected and eluted using a 20-min long gradient profile consisting of 0.1 % of formic acid (A) and 0.1 % of formic acid in methanol (B) at a 0.2 mL/min flow rate. The gradient profile started at 5 % B and increased to 95 % in 15 min. Detection of the alkylated polysulfur species were carried out by positive electrospray ionization and selected single reaction monitoring. The precursor → product mass transitions for HPE-IAM$_2$-S, HPE-IAM$_2$-S$_2$, HPE-IAM$_2$-S$_3$, HPE-IAM$_2$-S$_4$ and HPE-IAM$_2$-S$_5$ were 389 → 252, 421 → 212, 453 → 244, 485 → 276 and 517 → 308, respectively.

2.5. Protein structures

For the visualization of the structural features of proteins, the PyMOL Molecular Graphics System (Version 2.0 Schrödinger, LLC) was used.

3. Results and discussion

3.1. Interactions of ferric and ferrous LPO with H_2S under aerobic and anaerobic conditions

UV–vis spectral changes of LPO-Fe(III) during its reaction with excess sulfide under aerobic conditions are shown in Fig. 2A. Upon addition of excess sulfide, the Soret peak shifts from 412 nm to 418 nm and new bands at 547 nm, 587 nm, 638 nm and 727 nm replace the characteristic bands of LPO-Fe(III) at 501 nm, 541 nm, 589 nm and 631 nm [30]. The 638 nm and 727 nm transitions were tentatively assigned to ferrous sulfLPO-Fe(II) and ferric sulfLPO-Fe(III) species, respectively. Peak formations at around 547 nm and 587 nm and the transition of the Soret band to 418 nm were previously also observed in the aerobic reaction of LPO-Fe(III) with excess sulfide [41]. Interestingly these transitions resemble the characteristic peaks of Compound III (Soret peak: 423 nm, Q bands: 550 nm and 584 nm) [49].

In contrast, under strictly anaerobic conditions no spectral changes were observed by the stopped-flow technique within 100.0 s after mixing LPO-Fe(III) with excess sulfide (Fig. 2B). However, on a longer time scale under similar reaction conditions, the transformation of the LPO-Fe(III) UV–vis spectrum suggests a slow reaction between LPO-Fe(III) and H_2S, but no sulfheme formation (Fig. 2C). The red shift of the Soret peak and the evolution of the characteristic peaks of ferrous LPO-Fe(II) at 561 and 593 [49] suggest this reaction to be a sulfide-mediated partial reduction of LPO-Fe(III). Only the subsequent addition of O_2 to this mixture led to the appearance of the sulfLPO-Fe(II) and sulfLPO-Fe(III) peaks at 638 nm and 727 nm, respectively accompanied by a slight blue shift of the Soret peak to 415 nm. These data indicate the need for molecular dioxygen to produce these sulfLPO products (Fig. 2D).

Table 1
Reaction mixture compositions for polysulfide speciation.

	1	2	3	4	5
H_2S (μM)	1000	1000	1000	1000	1000
H_2O_2 (μM)	0	100	0	10	100
LPO (μM)	0	0	1	1	1

To further corroborate the O_2 requirement of the reaction, a similar experiment was conducted using preformed ferrous LPO-Fe(II). Ferrous LPO-Fe(II) was generated in the reaction of ferric LPO-Fe(III) and dithionite under anaerobic conditions followed by mixing with sulfide still in the absence of O_2 and finally, O_2 was added to the reaction mixture (Fig. 2E). The characteristic peaks of LPO-Fe(II) at 444 nm, 561 nm and 593 nm appeared upon the reduction of LPO-Fe(III) with dithionite [49]. Mixing sulfide with LPO-Fe(II) caused no spectral changes. However, the subsequent addition of O_2 to the reaction mixture resulted a characteristic 638 nm peak and the shift of the Soret peak to 424 nm, which was assigned to sulfLPO-Fe(II) [41]. Interestingly, the characteristic sulfLPO-Fe(III) band at 727 nm did not show up, which is in line with the previous assignments of these absorbance maxima.

In summary, our data indicate that for LPO the formation of the 638 nm and 727 nm derivatives directly depends on the presence of both O_2 and H_2S. Evolution of these characteristic sulfLPO peaks was observed in three different experimental setups: 1) sulfide was added to ferric LPO-Fe(III) in the presence of oxygen (Fig. 2A); 2) O_2 was added to the mixture of ferric LPO-Fe(III) and sulfide, in which ferrous LPO-Fe(II) was partially generated by slow sulfide-mediated LPO-Fe(III) reduction (Fig. 2C–D) and 3) O_2 was added to the mixture of preformed LPO-Fe(II) and H_2S (Fig. 2E). It is worth mentioning that the peak of sulfLPO-Fe(III) at 727 nm only appeared in the first two cases, when the reaction mixture contained the LPO-Fe(III) form.

3.2. Catalytic turnover of LPO with H_2O_2 in the presence of H_2S

Sulfide as an alternative substrate in the catalytic turnover of LPO by H_2O_2 was investigated (Fig. 3A–H). First, ferric LPO-Fe(III) was reacted with H_2O_2. After 2 min of incubation, sulfide was added to the sample in large excess. Upon a slow decline (minutes) of the 638 nm band, additional aliquots of fresh H_2O_2 were introduced to the reaction mixtures as indicated by the grey arrows in Fig. 3G. Changes in the adsorption spectra were followed by UV–vis spectroscopy.

Fig. 3A presents the characteristic band displacements from native ferric LPO-Fe(III) (412 nm, 501 nm, 541 nm, 589 nm and 631 nm) to oxo-ferryl heme species (Por-Fe(IV)═O) (430 nm, 535 nm and 567 nm) upon its reaction with a 5-fold excess of H_2O_2 [30,49]. Important to note that the oxo-ferryl species could represent Compound II (Por-Fe(IV)═O) or Compound I* ($^{+\bullet}$aa-Por-Fe(IV)═O) as the electron structure of the heme motif is the same in the two species and so their absorption spectra cannot be distinguished from each other. The addition of a 180-fold excess of H_2S to the oxo-ferryl derivative(s) resulted in the formation of ferrous sulfLPO-Fe(II) and ferric sulfLPO-Fe(III) (638 nm and 727 nm, respectively) (Fig. 3B). The following slight blue shift and intensity increase of the Soret band, as well as the significant decrease of the characteristic sulfLPO peak at 638 nm, and the peaks at 547 and 587 nm on the minutes timescale collectively indicated a slow decay of sulfLPO species, which is accompanied by the partial recovery of native LPO-Fe(III) (Fig. 3C). To further study the reversible nature of sulfLPO formation, an additional aliquot of H_2O_2 (10x of the LPO concentration) was added to this mixture containing the recovered native LPO-Fe(III) (Fig. 3D). It was expected, that sulfide was still in excess in this solution. Indeed, the typical characteristic peaks of sulfLPO were reformed upon the addition of the second H_2O_2 aliquot shown by the absorbance increases at 547, 587, and 638 nm. It should be noted that the dominance of the 638 nm peak in the Q band region is much more prominent in this case and the Soret peak shifts to 424 nm compared to those in Fig. 3B, which may indicate the dominance of the ferrous sulfLPO-Fe(II) species. Over time, the intensity of the sulfLPO peaks at 547, 587, and 638 nm drop again, and the Soret peak shifts to 416 nm again suggesting a slow recovery of LPO-Fe(III) (Fig. 3E).

The time-resolved changes in the characteristic sulfLPO peak intensity at 638 nm were followed upon repeated re-addition of H_2O_2 and subsequent incubation times as shown in Fig. 3G. The first 8 points in Fig. 3G were derived from the discussed adsorption spectra in the

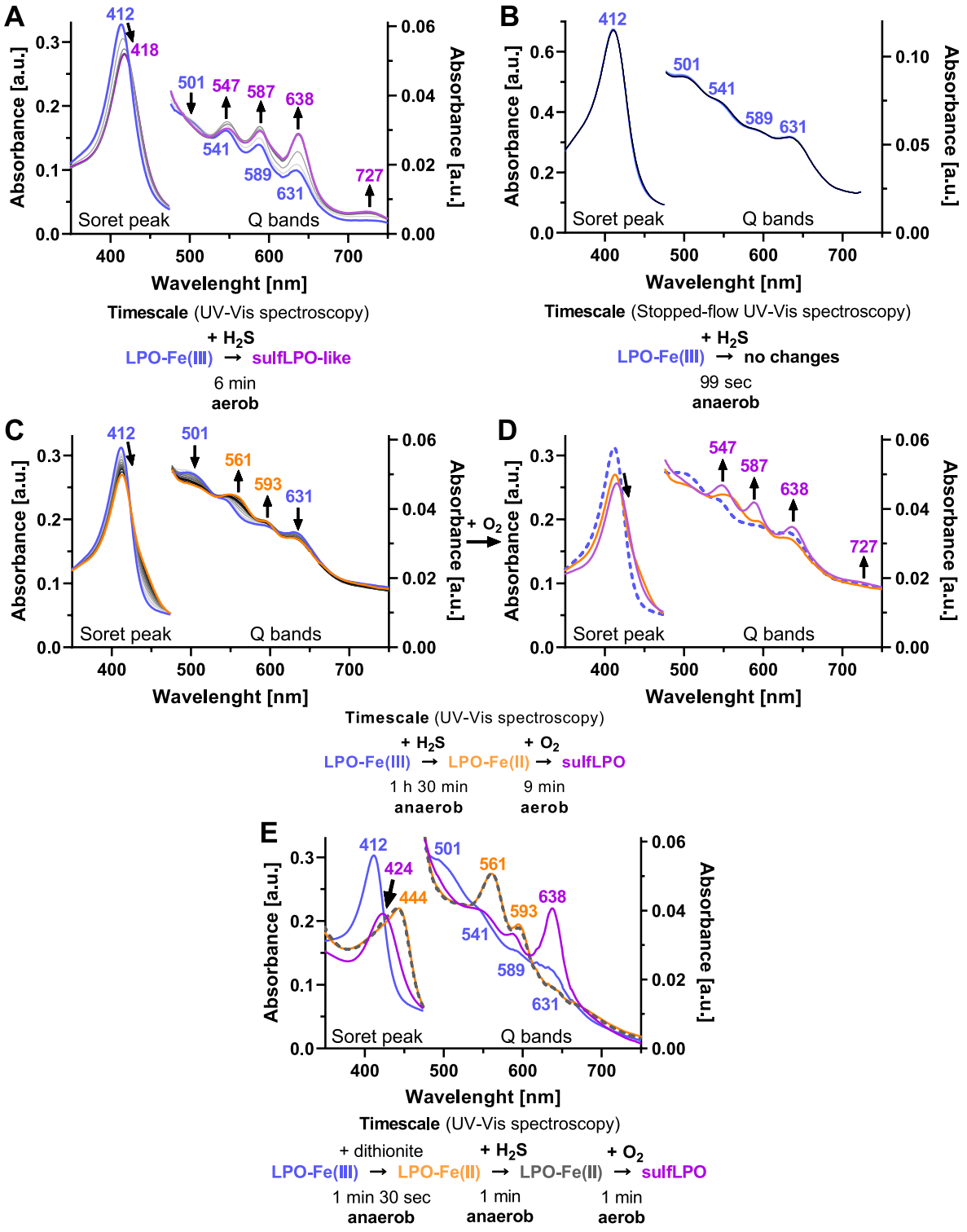

Fig. 2. UV–vis absorption spectral changes during the interactions of ferric LPO-Fe(III) and ferrous LPO-Fe(II) with H_2S in the absence and presence of O_2. A) Upon the addition of 150 μM H_2S to 3 μM LPO-Fe(III) under aerobic conditions, the characteristic bands of sulfLPO-Fe(III) and sulfLPO-Fe(II) emerged at 638 nm and 727 nm respectively (UV–vis spectra were recorded at 0.5 min, 1 min, 2 min, 4 min and 6 min after H_2S addition). B) 6 μM LPO-Fe(III) was reacted with 280 μM H_2S under anaerobic conditions and no spectral changes were observed within 100 s (UV–vis spectra were recorded at 0.81 s, 5.6 s, 9.3 s, 21.0 s, 30.0 s, 49.9 s, 69.1 s, 81.1 s, and 100.0 s with a stopped-flow instrument after mixing the reagents). C) Incubation of 2.7 μM LPO-Fe(III) with 150 μM H_2S under anaerobic conditions led to the partial generation of LPO-Fe(II) (UV–vis spectra were recorded every 5 min for 1.5 h). D) The introduction of O_2 to the system led to the partial formation of sulfLPO-Fe(II) with a characteristic band at 638 nm. E) 2.7 μM LPO-Fe(III) was reduced to LPO-Fe(II) using a seven-fold excess of dithionite under anaerobic conditions. Subsequent addition of 50 μM H_2S to the system led to no spectral changes in the absence of O_2. Upon introduction of O_2 to the mixture the characteristic peak of ferrous sulfLPO-Fe(II) emerged at 638 nm.

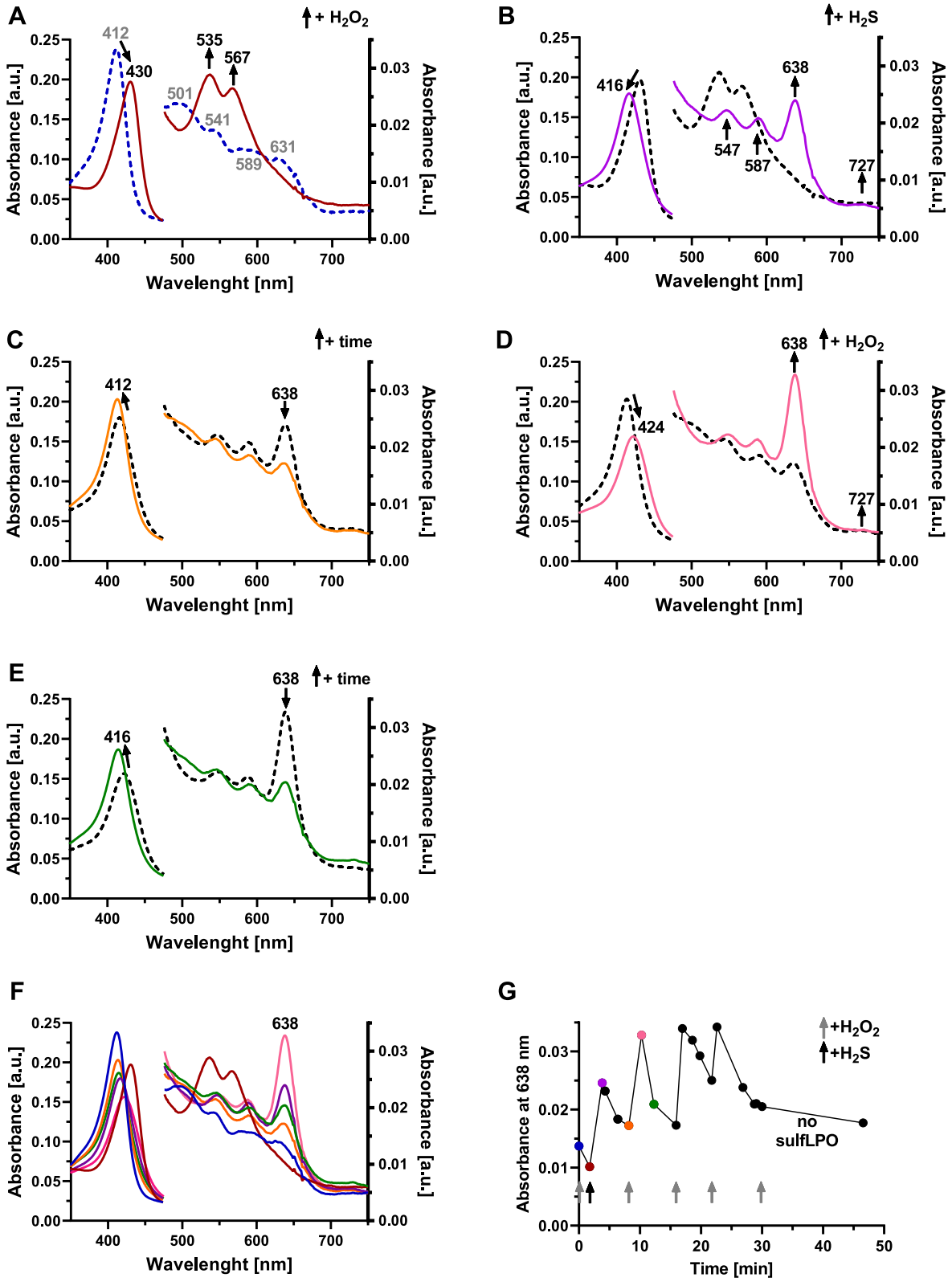

H

LPO-Fe(III) —(+ H_2O_2, A)→ Por-Fe(IV)=O —(+ H_2S, B)→ sulfLPO —(+ time, C)→ LPO-Fe(III) —(+ H_2O_2, D)→ sulfLPO —(+ time, E)→ LPO-Fe(III) —(+ H_2O_2, G)→ no sulfLPO

(caption on next page)

Fig. 3. Turnover of LPO in the presence of H_2O_2 and H_2S through intermediate formation of sulfLPO. For clarity, spectral changes upon sequential addition of reagents (+H_2O_2, +H_2S) (to the same reaction mixture) and during incubation periods (+time) between reagent addition steps are presented separately on A) – E). Dashed lines (– -) indicate the initial spectra of the corresponding reaction/incubation step and colored solid lines represent the final spectra before the next step in the sequence. Black arrows highlight the most relevant spectral transitions. A) Oxo-ferryl species (–) were generated by adding 10.5 μM H_2O_2 to 2.1 μM native LPO-Fe(III) (– -) and incubating for 2 min. B) Subsequent addition of 375 μM H_2S to this mixture (– -) generated sulfLPO (–). C) Over time spectral changes of the sulfLPO spectrum (– -) indicate the partial recovery of LPO-Fe(III) (–). D) At the 8. min another aliquot of 21 μM of H_2O_2 was added to the recovered LPO-Fe(III) (– -), which increased the intensity of the 638 nm band (–). E) After a short incubation period, the spectrum recorded at 12 min 30 s (–) shows a decrease of the band intensity at 638 nm and a blue shift of the Soret peak. F) Summarized spectral changes during the experiment separately shown on A) – E). G) Consecutive increase and decrease in the absorbance at 638 nm upon the addition of aliquots of H_2O_2 to the same mixture indicate turnover of LPO via intermediate formation of sulfLPO. Grey and black arrows indicate the H_2O_2 and H_2S addition steps, respectively. H) Schematic illustration of the reaction steps. The color code of the LPO derivatives represents the colors of the corresponding spectra on A) – G). (For interpretation of the references to color in this figure legend, the reader is referred to the Web version of this article.)

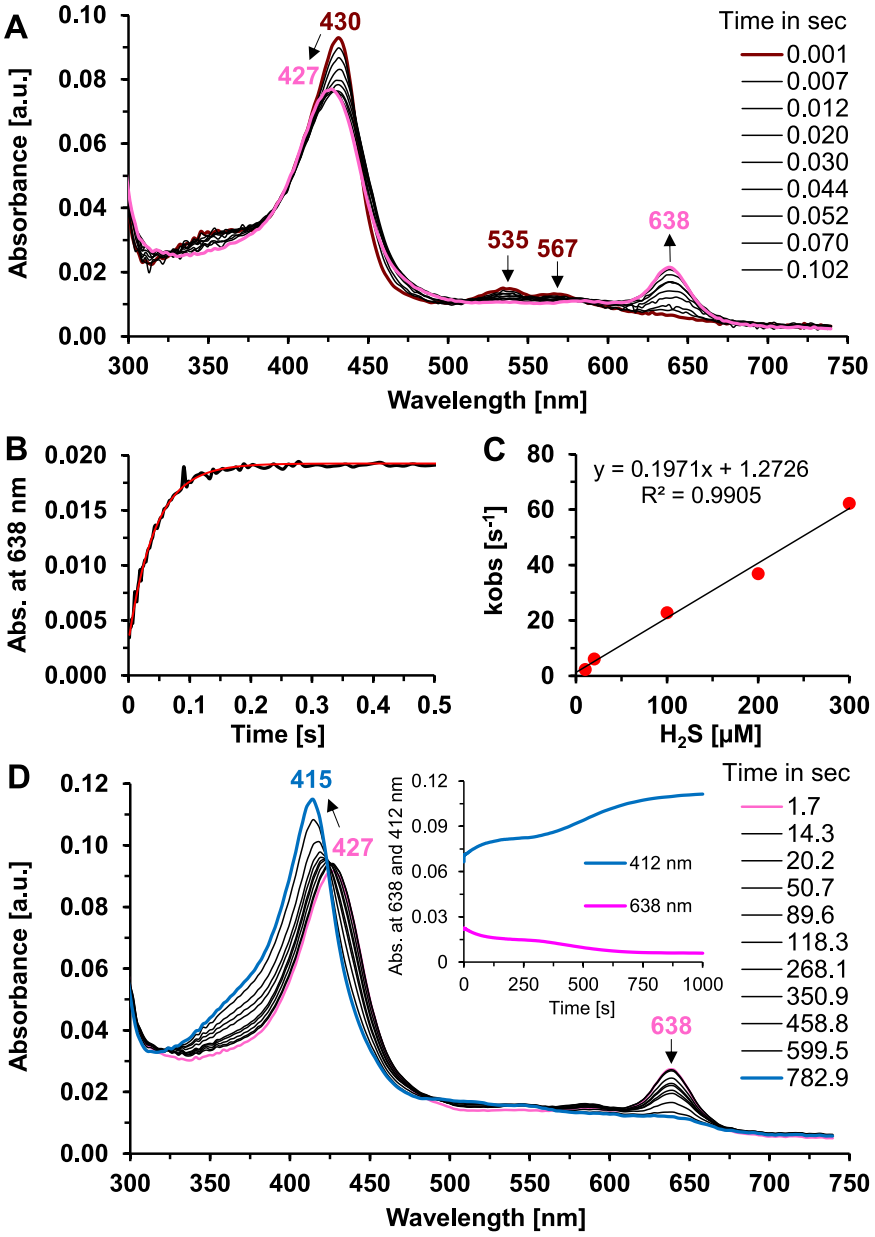

Fig. 4. Kinetic investigations for the reaction of LPO oxo-ferryl species with hydrogen sulfide using stopped-flow spectroscopy. A) Time-resolved spectral changes show sulfLPO formation (pink) in the reaction of 0.9 μM oxo-ferryl species (red) with 100 μM H_2S. B) Single exponential fit (red) to the kinetic time trace (black) of the characteristic sulfLPO peak evolution at 638 nm upon the addition of H_2S. C) Linear dependency of the obtained pseudo-first-order rate constants for sulfLPO formation on the H_2S concentration. D) The decay of sulfLPO (pink) was accompanied by the recovery of LPO-Fe(III) (blue) following the reaction of 1 μM LPO with 300 μM of H_2S; inset shows the characteristic Soret peak evolution at 412 nm (blue) and the parallel decay of the sulfLPO peak at 638 nm (pink). (For interpretation of the references to color in this figure legend, the reader is referred to the Web version of this article.)

previous section, summarized on Fig. 3F. Fig. 3G shows consecutive increase and decrease periods of the 638 nm band corresponding to H_2O_2 addition-induced sulfLPO formation and subsequent LPO-Fe(III) recovery, respectively. These data indicate a constant turnover of LPO via intermediate formation of sulfLPO upon the addition of H_2O_2 in the presence of excess H_2S. The repetitive addition of H_2O_2 was conducted until no intensity change was observable at the investigated wavelengths. The lack of sulfLPO formation upon the addition of the last H_2O_2 dose indicated the total consumption of sulfide. The repeated H_2O_2 aliquot addition to the mixture caused similar absorbance changes at 638 nm (Fig. 3G) until the consumption of H_2S, so we believe that after rapid conversion of the added H_2O_2 to sulfLPO formation, the enzyme slowly returns to a fully active form representing enzyme states before peroxide addition. This experiment was reproduced several times using different incubation times, with similar results (see e.g. Supplemental Fig. S2).

3.3. Reactivity of LPO oxo-ferryl species with H_2S

As mentioned above the oxo-ferryl species could represent Compound II (Por-Fe(IV)=O) or Compound I* ($^{+\bullet}$aa-Por-Fe(IV)=O) which cannot be distinguished spectroscopically. Nevertheless, we were interested in how fast this oxo-ferryl species reacts with H_2S. Fig. 4A shows the reaction of 0.9 μM oxo-ferryl species with 100 μM H_2S. Starting with the oxo-ferryl species with characteristic bands at 430 nm, 535 nm and 567 nm (red spectrum), we observed a transition with a marked increase at 638 nm and a decrease in the Soret band, representing the formation of sulfLPO (pink spectrum). A typical monophasic kinetic time trace at 638 with a single exponential fit is shown in Fig. 4B. The obtained pseudo-first-order rate constants showed a linear dependency on the H_2S concentration (Fig. 4C). The apparent second-order rate constants for the formation of sulfLPO were calculated from the slopes to be $1.79 \times 10^5\ M^{-1}\ s^{-1}$. As already shown in Fig. 3, sulfLPO was not stable and decayed to LPO-Fe(III). Fig. 4D shows the corresponding spectral changes and kinetic traces (inset) for the evolution of the Soret peak at 412 nm and the loss of the characteristic sulfLPO peak at 638 nm over a 13-min time period. SulfLPO decayed in a biphasic manner to LPO-Fe(III), where the slight shift in the Soret maximum from 412 nm to 415 nm is likely caused by the presence of a small amount of Compound III or another low spin species.

3.4. Investigation of enzyme forms during the catalytic reactions of LPO using H_2O_2 and H_2S as substrates

We used EPR spectroscopy to gain deeper insight into the nature of the enzyme forms in the reactions of LPO with H_2O_2 in the presence of H_2S. Fig. 5 compares the EPR spectra of native LPO-Fe(III) (Fig. 5A), the reaction mixture of LPO-Fe(III) and H_2O_2 (in 3-fold excess) (Fig. 5B) and the reaction mixture of LPO-Fe(III), H_2O_2 (in 3-fold excess) and equimolar (Fig. 5C) or 50-fold excess (Fig. 5D) of sulfide relative to the LPO concentration.

The EPR spectrum of native LPO-Fe(III) shows the characteristic high-spin ferric iron signal (Fig. 5A). Upon the addition of H_2O_2 a free radical peak also appeared with a g value of 2.004, which is characteristic of a carbon-centered radical (Fig. 5B). Previously this radical species was tentatively assigned to a tyrosyl radical derivative, which was generated from oxo-ferryl intermediates by intramolecular electron transfer [50]. The high-spin ferric signal remained transiently stable during the reactions of LPO-Fe(III) with H_2O_2, representing the resting state of the enzyme under these conditions.

The reactions of LPO with H_2O_2 in the presence of H_2S were carried out at two different concentration conditions with enzyme-to-substrate ratios of: LPO:H_2O_2:H_2S = 1:3:1 (Fig. 5C) or 1:3:50 (Fig. 5D). At the lower concentration of H_2S (Fig. 5C) the spectrum only shows a high-spin Fe(III) signal and no free radical peak at 2.004 g. This observation not necessarily means that the radical was not generated, but it certainly had a lifetime too short to be trapped in the timescale of sample mixing and freezing. This is consistent with the fact that H_2O_2 was applied in excess relative to both LPO and H_2S in this experiment and therefore, the observed high-spin ferric signal is most likely a result of rapid LPO catalyzed consumption of sulfide in its reactions with H_2O_2.

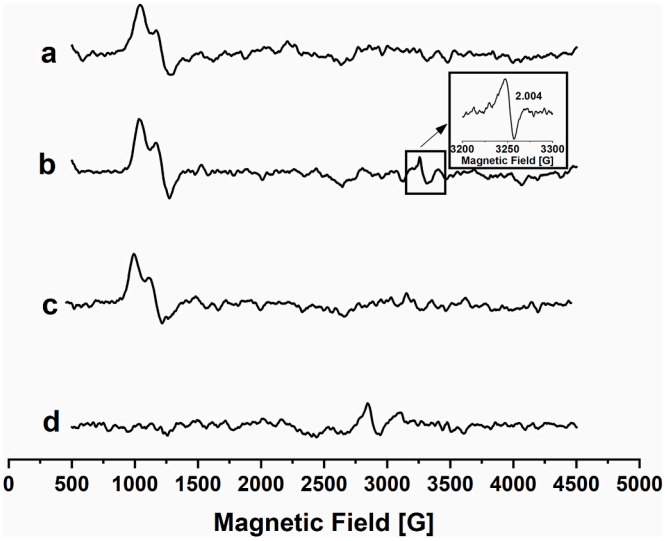

Fig. 5. EPR spectra upon the reactions of LPO with H_2O_2 and H_2S. EPR spectra of A) 300 μM ferric LPO-Fe(III), B) 300 μM ferric LPO-Fe(III) reacted with 900 μM H_2O_2, 300 μM ferric LPO-Fe(III) reacted with 900 μM H_2O_2 followed by the addition of C) 300 μM or D) 15000 μM H_2S. The inset shows an enhancement of the signal at the magnetic field range of 3200 G to 3300 G, which was assigned to an LPO tyrosyl radical (or other carbon-centered radical) species at 2.004 g.

At a 50-fold excess of H_2S, the spectrum (Fig. 5D) only shows a weak low-spin Fe(III) signal at 2.27 g. Based on the observed and reported [60] characteristic UV–vis bands at 727 nm, 416 nm, 547 nm and 587 nm (Fig. 3B) in a similar reaction mixture, we propose that this low-spin Fe(III) signal may be assigned to a sulfLPO(III)-oxygen complex. In agreement with this assignment, the observed g-value of 2.27 is similar to those reported for oxygenated Mb, horseradish peroxidase (HRP) and chloroperoxidase species [61]. The relatively low intensity of the signal is in line with the UV–vis spectrophotometry results (Fig. 3), where the formation of a mixture of ferrous (EPR silent) and ferric sulfLPO was observed under these reaction conditions. Moreover, the EPR spectra in the 2.004 g region indicated no detectable formation of the LPO tyrosyl radical species in the presence of sulfide at either condition (Fig. 5C and D).

3.5. Products of LPO catalyzed oxidation of H_2S with H_2O_2

Heme protein-mediated sulfide oxidation pathways resulting in sulfate, thiosulfate or polysulfide formation were reported in several studies [15]. For example, MPO produced polysulfide species in the presence of H_2O_2 and H_2S, albeit no sign of sulfheme intermediate could be observed in its catalytic turnover [17]. On the other hand, the sulfheme prosthetic group extracted from sulfmyoglobin decomposed to protohemin and SO_4^{2-} as major products by first-order kinetics [46]. Because peroxide-mediated turnover of LPO with other substrates shows similarities with MPO, but in the presence of sulfide the formation of sulfheme derivatives was proposed, which resembles more the reactions of myoglobin under these conditions, we investigated the formations of sulfate and sulfane sulfur species in LPO catalyzed sulfide oxidation reactions. Fig. 6A shows an increase in sulfate production as a function of the initial sulfide concentration with 5 μM native LPO and 25 μM or 50 μM H_2O_2 using three different concentrations of H_2S: 600 μM, 800 μM and 1000 μM.

In addition, Fig. 6B shows a H_2O_2 concentration-dependent increase

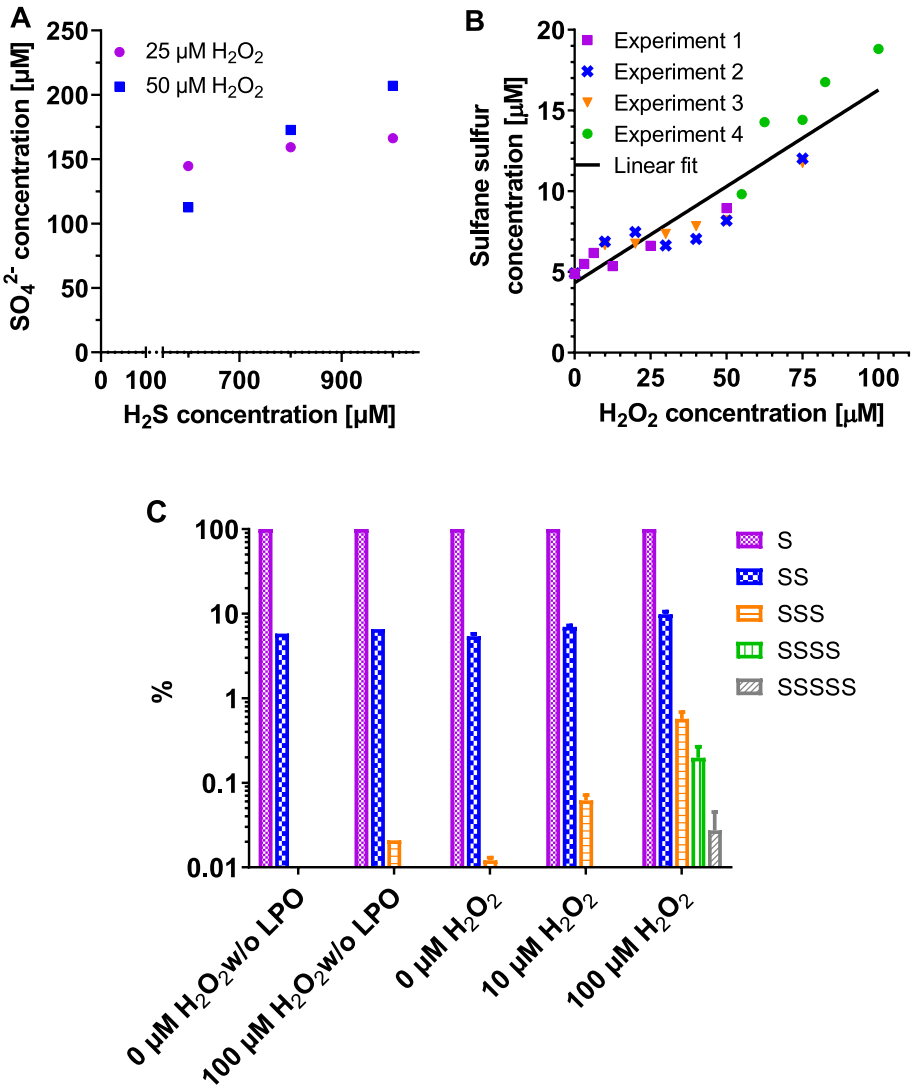

Fig. 6. Products of LPO catalyzed oxidation of H_2S with H_2O_2: A) Measured sulfate concentrations in the reactions of 5 μM ferric LPO, 600 μM (black), 800 μM (dark grey) or 1000 μM (grey) H_2S and 25 μM or 50 μM H_2O_2. B) Sulfane sulfur detection with SSP4 at 30 min in the reactions of 500 nM LPO, 5 mM H_2S as a function of the added H_2O_2 concentration. The observed linear correlation implies that ~12% of the H_2O_2 was converted to sulfane sulfur production. The differently labelled data sets represent individual experiments on different days using freshly prepared solutions C) Production of inorganic polysulfide species by LPO as a function of H_2O_2 concentration. 1 mM of HS^- was incubated with 1 μM of LPO for 30 min at 37 °C in the presence or absence of H_2O_2. After alkylation, polysulfide species were measured by HPLC-MS and levels were normalized to the HPE-IAM$_2$-S species (representing sulfide and depicted on the graph as "S") in each experiment. Disulfide species detected in the sample, which contains no LPO represent the disulfide contamination of the sulfide solution. In the absence of peroxide, LPO-induced measurable trisulfide production is likely due to H_2O_2 contamination in buffer solutions.

in sulfane sulfur production detected by the sulfane sulfur-specific fluorescent probe SSP4. Sulfane sulfur refers to sulfur atoms with 0 oxidation state (S^0). Semi-quantitative analyses of the signals using a calibration curve that was developed using known concentrations of inorganic polysulfide species suggested that approximately 12 % of the peroxide was converted to sulfane sulfur formation. In the absence of H_2O_2, a small amount of sulfane sulfur production was observed, which was also the case with MPO [17], but to a lesser extent in this case. Using mass spectrometry, we identified the formation of inorganic polysulfides representing a series of sulfane sulfur species. Fig. 6C shows the detected inorganic polysulfides with different chain lengths in the reactions of 1 mM sulfide with 0, 10 and 100 μM H_2O_2 in the presence of 1 μM LPO after alkylation with HPE-IAM and HPLC separation. The figure shows a normalized distribution of polysulfide species as % of remaining H_2S (shown as S1 and set at 100% assuming that it stayed constant due to its high excess) after 30 min incubation at 37 °C as a function of the H_2O_2 concentration. H_2O_2 alone (last group, no LPO) produced some S3 but LPO clearly had a catalytic effect on the reaction. In its presence, more and longer polysulfides were generated in a peroxide concentration-dependent manner.

4. Discussion

The reactions of H_2S with hemeproteins are in the focus of sulfide biology research [15]. In the presence of O_2 or H_2O_2, the reactions of sulfide with heme prosthetic groups in a number of different proteins were shown to produce the corresponding sulfheme derivatives [12,17,35,42,46,51–53]. Sulfheme formation reactions in most cases were reported to lead to loss of function (e.g. in the case of Hb [54] or Mb [55]). In some cases, sulfheme formation was not observed (for MPO), instead, these proteins catalyzed the oxidation of sulfide by H_2O_2. Interestingly, LPO was previously proposed to form sulfheme derivatives, albeit with relatively short lifetimes. Motivated by these observations in this study we tried to gain further insights into the reactions of sulfide with LPO

under different conditions.

4.1. Insights into the reactions of LPO with H_2S in the presence and absence of O_2

Under anaerobic conditions, we observed the reduction of the LPO heme iron in the presence of excess H_2S without any sulfLPO formation. This observation was confirmed by no detectable changes in the UV–vis spectrum upon the addition of sulfide to ferrous LPO-Fe(II) in the absence of O_2, which also suggested that H_2S has little (if any) coordinating affinity to the ferrous form of the iron center. However, H_2S reacted with native ferric or ferrous LPO in the presence of oxygen to generate products with characteristic UV–vis bands at 638 nm and 727 nm, which were previously assigned to the ferrous sulfheme and ferric sulfheme derivatives, respectively [41]. In previous studies using SCN^-, Br^- or Cl^- instead of H_2S under similar conditions, the appearance of these characteristic bands was not observed [56]. It should also be emphasized that Mb and Hb sulfheme derivatives have absorbance maxima in the same region at 620 nm and 717 nm, respectively and their formation also relies on the combined presence of O_2 and H_2S. These apparent similarities in the Q region of the optical absorbance spectra could suggest that the modification in the LPO heme may be a chlorin-type structure in which the sulfur atom is incorporated across the β-β double bond of the pyrrole B as in sulfHb or sulfMb [41,53,57].

4.2. Insights into the LPO-catalyzed oxidation of H_2S with H_2O_2

The reaction of LPO-Fe(III) with H_2O_2 results in the immediate formation of an LPO oxo-ferryl species (spectroscopically indistinguishable Compound II and/or Compound I*). Subsequent reaction of this oxo-ferryl species with hydrogen sulfide resulted in sulfLPO formation. The apparent second-order rate constant for this interaction was determined to be $1.79 \times 10^5\ M^{-1}\ s^{-1}$. SulfLPO decays in a biphasic manner to LPO-Fe(III).

In addition, the reactions of LPO-Fe(III) with H_2O_2 in the presence of excess H_2S resulted in a rapid formation of sulfLPO. The generated sulfLPO decayed in a minute timescale to recover LPO-Fe(III). Repeated addition of H_2O_2 consumed the total amount of H_2S demonstrating that in the presence of H_2O_2, H_2S serves as a non-classical LPO substrate, which turns over the enzyme with the intermediate formation of sulfheme derivatives. Interestingly, EPR data indicated that the presence of sulfide can prevent the formation of long-lived aromatic amino acid radicals on LPO during turnover.

4.3. Mechanistic considerations for sulfheme formation and decomposition

The ability of LPO to catalyze the oxidation of sulfide by H_2O_2 despite the apparent formation of sulfheme derivatives is in contrast to other systems where sulfheme formation inactivated enzymatic functions [12,34,40,41,43,51,52]. Therefore, this unique feature deserves attention from the mechanistic point of view. Previous data indicate that the orientation and position of the His residue at the heme active site are crucial factors in the formation of sulfheme products. Site-directed mutagenesis in hemoglobin I, where His 64 was replaced with Arg diminished sulfheme formation [12,35]. With the exception of a limited group of heme proteins, such as cytochrome *c* oxidase [58], HRP [51], MPO [17] or the phosphodiesterase His mutant (Ec DOS-PAS Met95His) [59] which do not form sulfheme, the distal His seems to be able to promote the formation of the corresponding sulfheme derivatives [12,35]. It was proposed that in MPO a bow-shape distortion of the heme displaces the iron center from the distal His, which could explain the loss of MPO's ability to form a sulfheme derivative [17]. Fig. 7 shows that the distal His in HRP is also further away from the iron center (6.0 Å) compared to in LPO (5.1 Å), which may contribute to the fact that LPO can, but HRP cannot produce a sulfheme derivative [12,51].

Although our studies were not strictly mechanistic in the sense of sulfheme formation, based on previous literature data we attempt to speculate how sulfLPO might form in the presence of hydrogen peroxide or oxygen. These speculative pathways are shown in Fig. 8. Fig. 8A shows the proposed reactions with peroxide, which is based on the recent DFT/MM potential energy scans method coupled to the CHARMM force field, indicating hydrogen transfer from H_2S to Fe(III)–H_2O_2 followed by homolytic cleavage of the O–O and S–H bonds to form $^{\bullet}SH$, Compound II, and a water molecule [42]. Subsequent addition of $^{\bullet}SH$ to a pyrrole B carbon of Compound II leads to a 3-membered episulfide ring and met-aqua Fe(III). Finally, the energetically favourable 5-membered thiochlorin structure could form from the 3-membered episulfide ring [42]. In the case of LPO and O_2, it was shown that Compound III (Por-Fe(II)–O_2/Por-Fe(III)–$O_2^{\bullet-}$) can accept an electron and a proton to form Compound 0 and His109 plays an important role in this process [31]. Therefore, Fig. 8B suggests that sulfide-induced sulfheme formation in LPO may go through Compound III and Compound 0 in the presence of dioxygen. It is suggested that Compound III could accept an electron and a proton from H_2S, which in turn could undergo a homolytic cleavage [42] Compound III could thus be transformed to Compound 0, a Por-Fe(III)-hydroperoxo bound state and $^{\bullet}SH$, which subsequently could induce heterolytic peroxide bond cleavage to give Compound I and release water. Subsequent recombination of Compound I and $^{\bullet}SH$ could then lead to the formation of sulfLPO. Of note, oxyMb can also form Compound III [31,61,62] and previous studies

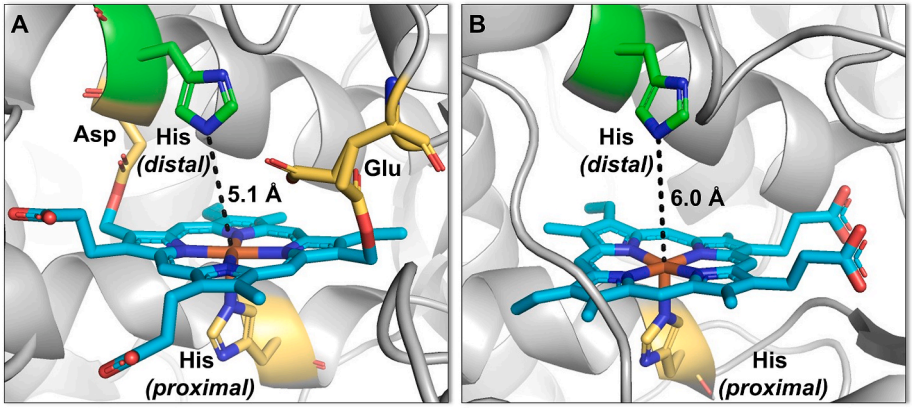

Fig. 7. Distal active site of (A) LPO (PDB:5b72) [32] and (B) HRP (PDB:1ATJ) [60]. Cyan blue: carbon in porphyrin (Por); yellow: carbon in heme binding protein residues (His: proximal histidine, Glu: glutamic acid, Asp: aspartic acid); green: carbon in distal His residues; orange: iron ion; red: oxygen; dark blue: nitrogen. (For interpretation of the references to color in this figure legend, the reader is referred to the Web version of this article.)

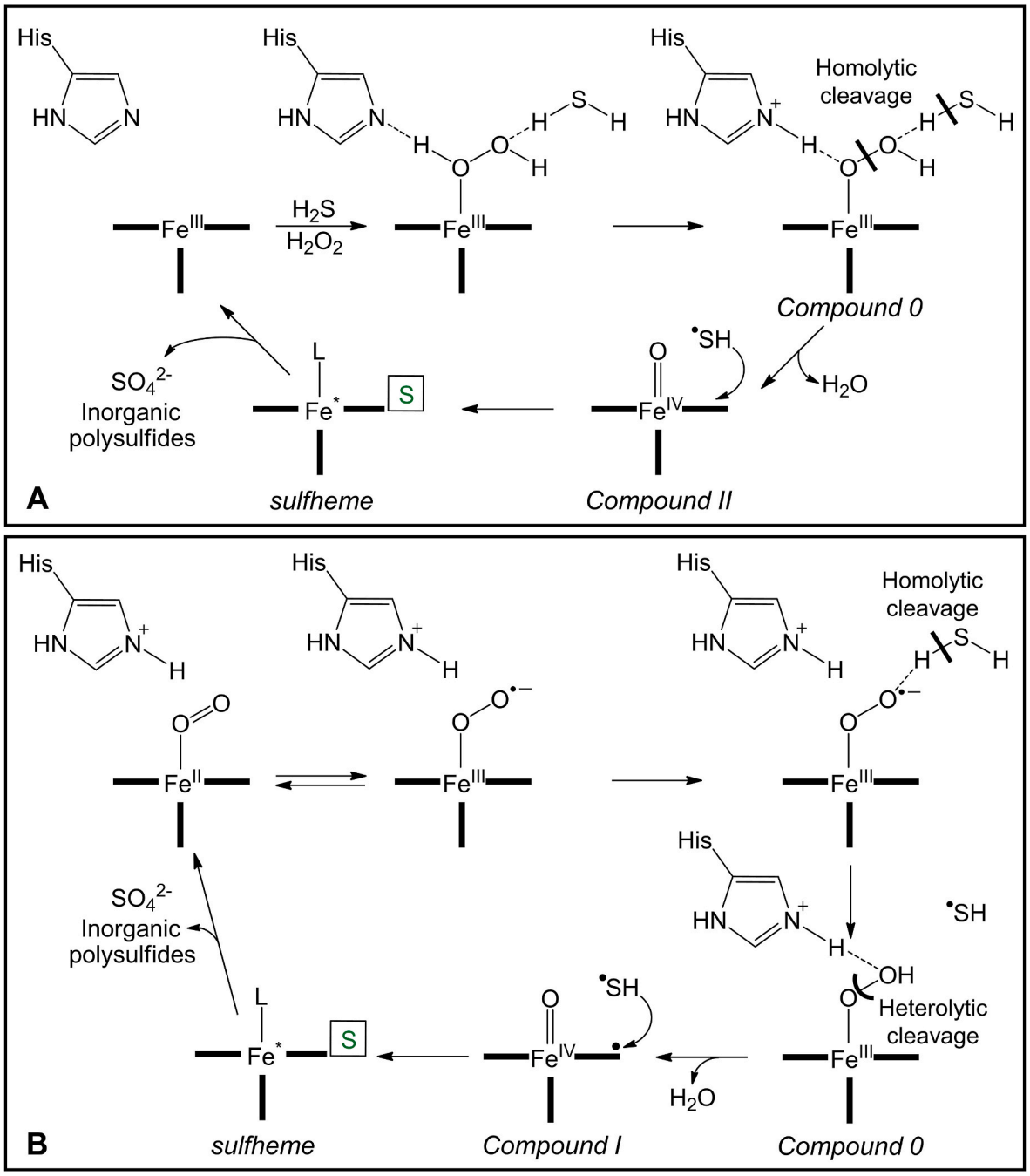

Fig. 8. Proposed mechanism for sulfheme formation of LPO and H_2S in the presence of (A) hydrogen peroxide and (B) oxygen.

suggest that the •SH radical in this case is also involved in sulfheme formation [12,35,42,51,63]. In the proposed mechanisms for the sulfheme formation with O_2 or H_2O_2, the rate-limiting steps are likely to be the generation of Compound III or Compound 0, respectively. While the suggested mechanism is speculative and additional experiments are needed to support this theory, we believe that it reasonably summarizes the current knowledge on sulfLPO formation and could give a valuable perspective for further research.

The concept of reversion of sulfheme to the corresponding native protein is not new, in fact, this was observed in proteins such as Mb, Hb, and catalase under different experimental conditions [40,51,64,65]. However, LPO seems to be unique among peroxidases with its rapid rate of sulfLPO turnover as a catalytic intermediate (as opposed to a long-lived dead-end inhibitory species). Previous literature data [66–68] indicates that desulfurization of alkyl and organic aromatic sulfides in the presence of oxidizing agents, such as O_2 or H_2O_2, leads to the production of sulfate [69,70]. In fact, an early work on sulfMb, using radioactive ^{35}S, indicated that the decomposition of the isolated sulfheme motif produces sulfate as the major product, while the formations of H_2S, SO_2 and elemental sulfur were ruled out [46]. We obtained data suggesting an increase in LPO-induced sulfate production in the presence of H_2O_2 in a H_2S concentration-dependent manner. Approximately 20 % of the initially added H_2S were estimated to be converted to sulfate.

In addition to sulfate, we showed evidence for the formation of inorganic polysulfide species in this system, which accounted for approximately 12% of the added H_2O_2. One could speculate that inorganic polysulfides could be generated by the escape of thyil radicals

from the active site and sulfate may be the product of sulfheme turnover. However, our data provide no insights into the contributions of these pathways. It also has to be noted that upon acidification of the reaction mixtures, polysulfides could precipitate as S_8, which could contribute to the increase in turbidity in the barium-sulfate assay for sulfate measurement [6,71,72].

Future studies regarding the physiological relevance of LPO and sulfLPO turnover

The *in vitro* results, we presented here may pave the way for future investigations to support the suggested mechanism with carefully conducted *in vitro* kinetical studies, including the determination of kinetic parameters, and thereby contribute to our understanding regarding the anti-inflammatory and antioxidant functions of LPO and H_2S in airways [73]. Furthermore, our results may initiate *in vivo* studies to assess the ability of LPO to use H_2S as substrate and generate bioactive inorganic polysulfides as products *in vivo* or the potential role of H_2S in preventing carbon center radical formation on LPO during H_2O_2 scavenging. For example, H_2O_2 depletion by LPO via sulfheme formation may open new avenues to investigate the *in vivo* prevention of the toxic effects of H_2O_2 in patients with asthma and COPD or in the crosstalk between LPO and cystathionine β-synthase and/or cystathionine γ-lyase enzymes in the antioxidant character of H_2S. Regarding the toxic nature of H_2S [74], upon inhalation of relatively high concentrations, LPO may serve as a "H_2S sink" to protect mammals from sulfide toxicity.

CRediT authorship contribution statement

Bessie B. Ríos-González: Conceptualization, Investigation, Writing – original draft. **Andrea Domán:** Validation, Visualization, Writing – original draft, Writing – review & editing. **Tamás Ditrói:** Investigation. **Dorottya Garai:** Investigation. **Leishka D. Crespo:** Conceptualization, Investigation. **Gary J. Gerfen:** Conceptualization, Funding acquisition, Investigation. **Paul G. Furtmüller:** Conceptualization, Investigation, Resources. **Péter Nagy:** Conceptualization, Funding acquisition, Resources, Supervision, Writing – original draft. **Juan López-Garriga:** Conceptualization, Funding acquisition, Resources, Supervision, Writing – original draft.

Declaration of competing interest

The authors declare that they have no known competing financial interests or personal relationships that could have appeared to influence the work reported in this paper.

Acknowledgements

This work was supported in part by NIH-RISE (Grant R25GM088023) and the National Science Foundation (Grant 0843608 to J.L.G. and CHE-1213550 to G.J.G.). The project was implemented with the support from the National Research, Development and Innovation Fund of the Ministry of Culture and Innovation under the National Laboratories Program (National Tumor Biology Laboratory (2022–2.1.1-NL-2022-00010 to P. N.)) and the Hungarian Thematic Excellence Program (under project TKP2021-EGA-44 to P.N.) Grant Agreements with the National Research, Development and Innovation Office. This project has received funding from the HUN-REN Hungarian Research Network (grant 1500207 to P.N.). We thank Dr. Syun-Ru Yeh for the stopped-flow instrument use and Ariel Lewis-Ballester for the assistance with it. Also, we thank Beatriz Muñoz and Darya Marchany for the assistance.

Appendix A. Supplementary data

Supplementary data to this article can be found online at https://doi.org/10.1016/j.rbc.2024.100021.

References

[1] O. Kabil, R. Banerjee, Enzymology of H_2S biogenesis, decay and signaling, Antioxidants Redox Signal. 20 (5) (2014) 770–782, https://doi.org/10.1089/ars.2013.5339.
[2] P. Nagy, Z. Pálinkás, A. Nagy, B. Budai, I. Tóth, Vasas, Chemical aspects of hydrogen sulfide measurements in physiological samples, Biochim. Biophys. Acta, Gen. Subj. 1840 (2) (2014) 876–891, https://doi.org/10.1016/j.bbagen.2013.05.037.
[3] K. Abe, H. Kimura, The possible role of hydrogen sulfide as an endogenous neuromodulator, J. Neurosci. 16 (3) (1996) 1066–1071, https://doi.org/10.1523/jneurosci.16-03-01066.1996.
[4] L. Li, P. Rose, P.K. Moore, Hydrogen sulfide and cell signaling, Annu. Rev. Pharmacol. Toxicol. 51 (1) (2011) 169–187, https://doi.org/10.1146/annurev-pharmtox-010510-100505.
[5] K. Ono, T. Akaike, T. Sawa, Y. Kumagai, D.A. Wink, D.J. Tantillo, A.J. Hobbs, P. Nagy, M. Xian, J. Lin, J.M. Fukuto, Redox chemistry and chemical biology of H_2S, hydropersulfides, and derived species: implications of their possible biological activity and utility, Free Radic. Biol. Med. 77 (2014) 82–94, https://doi.org/10.1016/j.freeradbiomed.2014.09.007.
[6] P. Nagy, Mechanistic chemical perspective of hydrogen sulfide signaling, Methods Enzymol. 554 (2015) 3–29, https://doi.org/10.1016/bs.mie.2014.11.036.
[7] C. Szabo, A timeline of hydrogen sulfide (H_2S) research: from environmental toxin to biological mediator, Biochem. Pharmacol. 149 (2018) 5–19, https://doi.org/10.1016/j.bcp.2017.09.010.
[8] G. Cirino, C. Szabo, A. Papapetropoulos, Physiological roles of hydrogen sulfide in mammalian cells, tissues, and organs, Physiol. Rev. 103 (1) (2023) 31–276, https://doi.org/10.1152/physrev.00028.2021.
[9] B.D. Paul, S.H. Snyder, H_2S signalling through protein sulfhydration and beyond, Nat. Rev. Mol. Cell Biol. 13 (8) (2012) 499–507, https://doi.org/10.1038/nrm3391.
[10] H. Kimura, Signaling molecules: hydrogen sulfide and polysulfide, Antioxidants Redox Signal. 22 (5) (2015) 362–376, https://doi.org/10.1089/ars.2014.5869.
[11] R. Pietri, E. Román-Morales, J. López-Garriga, Hydrogen sulfide and hemeproteins: knowledge and mysteries, Antioxidants Redox Signal. 15 (2) (2011) 393–404, https://doi.org/10.1089/ars.2010.3698.
[12] B.B. Ríos-González, E.M. Román-Morales, R. Pietri, J. López-Garriga, Hydrogen sulfide activation in hemeproteins: the sulfheme scenario, J. Inorg. Biochem. 133 (2014) 78–86, https://doi.org/10.1016/j.jinorgbio.2014.01.013.
[13] F.M. Boubeta, S.A. Bieza, M. Bringas, J.C. Palermo, L. Boechi, D.A. Estrin, S.E. Bari, Hemeproteins as targets for sulfide species, Antioxidants Redox Signal. 32 (4) (2020) 247–257, https://doi.org/10.1089/ars.2019.7878.
[14] J.J. Woods, J.J. Wilson, Bioinorganic Chemistry of Hydrogen Sulfide: Detection, Delivery, and Interactions with Metalloproteins, Encyclopedia of Inorganic and Bioinorganic Chemistry, 2021, pp. 1–22.
[15] A. Domán, É. Dóka, D. Garai, V. Bogdándi, G. Balla, J. Balla, P. Nagy, Interactions of reactive sulfur species with metalloproteins, Redox Biol. 60 (2023) 102617, https://doi.org/10.1016/j.redox.2023.102617.
[16] Z. Pálinkás, P.G. Furtmüller, A. Nagy, C. Jakopitsch, K.F. Pirker, M. Magierowski, K. Jasnos, J.L. Wallace, C. Obinger, P. Nagy, Interactions of hydrogen sulfide with myeloperoxidase, Br. J. Pharmacol. 172 (6) (2015) 1516–1532, https://doi.org/10.1111/bph.12769.
[17] D. Garai, B.B. Ríos-González, P.G. Furtmüller, J.M. Fukuto, M. Xian, J. López-Garriga, C. Obinger, P. Nagy, Mechanisms of myeloperoxidase catalyzed oxidation of H_2S by H_2O_2 or O_2 to produce potent protein Cys-polysulfide-inducing species, Free Radic. Biol. Med. 113 (2017) 551–563, https://doi.org/10.1016/j.freeradbiomed.2017.10.384.
[18] L. Potor, P. Nagy, G. Méhes, Z. Hendrik, V. Jeney, D. Pethő, A. Vasas, Z. Pálinkás, E. Balogh, Á. Gyetvai, M. Whiteman, R. Torregrossa, M.E. Wood, S. Olvasztó, P. Nagy, G. Balla, J. Balla, Hydrogen sulfide abrogates hemoglobin-lipid interaction in atherosclerotic lesion, Oxid. Med. Cell. Longev. 2018 (2018) 3812568, https://doi.org/10.3390/antiox12040868.
[19] H.B. Dunford, Heme Peroxidases, Wiley, 1999.
[20] P.G. Furtmüller, M. Zederbauer, W. Jantschko, J. Helm, M. Bogner, C. Jakopitsch, C. Obinger, Active site structure and catalytic mechanisms of human peroxidases, Arch. Biochem. Biophys. 445 (2) (2006) 199–213, https://doi.org/10.1016/j.abb.2005.09.017.
[21] M. Zámocký, S. Hofbauer, I. Schaffner, B. Gasselhuber, A. Nicolussi, M. Soudi, K. F. Pirker, P.G. Furtmüller, C. Obinger, Independent evolution of four heme peroxidase superfamilies, Arch. Biochem. Biophys. 574 (2015) 108–119, https://doi.org/10.1016/j.abb.2014.12.025.
[22] K.D. Kussendrager, A.C. van Hooijdonk, Lactoperoxidase: physico-chemical properties, occurrence, mechanism of action and applications, Br. J. Nutr. 84 (Suppl 1) (2000) S19–S25, https://doi.org/10.1017/s0007114500002208.
[23] C. Wijkstrom-Frei, S. El-Chemaly, R. Ali-Rachedi, C. Gerson, M.A. Cobas, R. Forteza, M. Salathe, G.E. Conner, Lactoperoxidase and human airway host defense, Am. J. Respir. Cell Mol. Biol. 29 (2) (2003) 206–212, https://doi.org/10.1165/rcmb.2002-0152OC.
[24] J.W. Boots, R. Floris, Lactoperoxidase: from catalytic mechanism to practical applications, Int. Dairy J. 16 (11) (2006) 1272–1276, https://doi.org/10.1016/j.idairyj.2006.06.019.
[25] G. Sievers, Structure of milk lactoperoxidase. A study using circular dichroism and difference absorption spectroscopy, Biochim. Biophys. Acta Protein Struct. 624 (1) (1980) 249–259, https://doi.org/10.1016/0005-2795(80)90244-5.

[26] P.G. Furtmüller, W. Jantschko, G. Regelsberger, C. Jakopitsch, J. Arnhold, C. Obinger, Reaction of lactoperoxidase compound I with halides and thiocyanate, Biochemist 41 (39) (2002) 11895–11900, https://doi.org/10.1021/bi026326x.
[27] A.K. Singh, N. Pandey, M. Sinha, P. Kaur, S. Sharma, T.P. Singh, Structural evidence for the order of preference of inorganic substrates in mammalian heme peroxidases: crystal structure of the complex of lactoperoxidase with four inorganic substrates, SCN, I, Br and Cl, Int. J. Biochem. Mol. Biol. 2 (4) (2011) 328–339.
[28] S. Sharma, A.K. Singh, S. Kaushik, M. Sinha, R.P. Singh, P. Sharma, H. Sirohi, P. Kaur, T.P. Singh, Lactoperoxidase: structural insights into the function,ligand binding and inhibition, Int. J. Biochem. Mol. Biol. 4 (3) (2013) 108–128.
[29] J. Vlasits, C. Jakopitsch, M. Bernroitner, M. Zamocky, P.G. Furtmüller, C. Obinger, Mechanisms of catalase activity of heme peroxidases, Arch. Biochem. Biophys. 500 (1) (2010) 74–81, https://doi.org/10.1016/j.abb.2010.04.018.
[30] E. Ghibaudi, E. Laurenti, Unraveling the catalytic mechanism of lactoperoxidase and myeloperoxidase, Eur. J. Biochem. 270 (22) (2003) 4403–4412, https://doi.org/10.1046/j.1432-1033.2003.03849.x.
[31] P.J. Mak, W. Thammawichai, D. Wiedenhoeft, J.R. Kincaid, Resonance Raman spectroscopy reveals pH-dependent active site structural changes of lactoperoxidase compound 0 and its ferryl heme O–O bond cleavage products, J. Am. Chem. Soc. 137 (1) (2015) 349–361, https://doi.org/10.1021/ja5107833.
[32] P.K. Singh, H.V. Sirohi, N. Iqbal, P. Tiwari, P. Kaur, S. Sharma, T.P. Singh, Structure of bovine lactoperoxidase with a partially linked heme moiety at 1.98Å resolution, Biochim. Biophys. Acta, Proteins Proteomics 1865 (3) (2017) 329–335, https://doi.org/10.1016/j.bbapap.2016.12.006.
[33] G. Rita, The use of spectrophotometry UV-vis for the study of porphyrins, in: U. Jamal (Ed.), Macro to Nano Spectroscopy, IntechOpen, Rijeka, 2012. Ch. 6.
[34] H.O. Michel, A study of sulfhemoglobin, J. Biol. Chem. 126 (1) (1938) 323–348, https://doi.org/10.1016/S0021-9258(18)73923-9.
[35] E. Román-Morales, R. Pietri, B. Ramos-Santana, S.N. Vinogradov, A. Lewis-Ballester, J. López-Garriga, Structural determinants for the formation of sulfhemeprotein complexes, Biochem. Biophys. Res. Commun. 400 (4) (2010) 489–492, https://doi.org/10.1016/j.bbrc.2010.08.068.
[36] H.D. Arbelo-López, A.D. Rodriguez-Mackenzie, E.M. Roman-Morales, T. Wymore, J. López-Garriga, Charge transfer and π to π* transitions in the visible spectra of sulfheme met isomeric structures, J. Phys. Chem. B 122 (19) (2018) 4947–4955, https://doi.org/10.1021/acs.jpcb.7b12393.
[37] J.A. Berzofsky, J. Peisach, W.E. Blumberg, I.I. Sulfheme proteins, The reversible oxygenation of ferrous sulfmyoglobin, J. Biol. Chem. 246 (23) (1971) 7366–7372.
[38] S.H. Libardi, H. Pindstrup, D.R. Cardoso, L.H. Skibsted, Reduction of ferrylmyoglobin by hydrogen sulfide. Kinetics in relation to meat greening, J. Agric. Food Chem. 61 (11) (2013) 2883–2888, https://doi.org/10.1021/jf305363e.
[39] P. Nicholls, The formation and properties of sulphmyoglobin and sulphcatalase, Biochem. J. 81 (2) (1961) 374–383, https://doi.org/10.1042/bj0810374.
[40] D. Padovani, A. Hessani, F.T. Castillo, G. Liot, M. Andriamihaja, A. Lan, C. Pilati, F. Blachier, S. Sen, E. Galardon, I. Artaud, Sulfheme formation during homocysteine S-oxygenation by catalase in cancers and neurodegenerative diseases, Nat. Commun. 7 (1) (2016) 13386, https://doi.org/10.1038/ncomms13386.
[41] S. Nakamura, M. Nakamura, I. Yamazaki, M. Morrison, Reactions of ferryl lactoperoxidase (compound II) with sulfide and sulfhydryl compounds, J. Biol. Chem. 259 (11) (1984) 7080–7085.
[42] H.D. Arbelo-Lopez, N.A. Simakov, J.C. Smith, J. Lopez-Garriga, T. Wymore, Homolytic cleavage of both heme-bound hydrogen peroxide and hydrogen sulfide leads to the Formation of sulfheme, J. Phys. Chem. B 120 (30) (2016) 7319–7331, https://doi.org/10.1021/acs.jpcb.6b02839.
[43] R.J. Carrico, W.E. Blumberg, J. Peisach, The reversible binding of oxygen to sulfhemoglobin, J. Biol. Chem. 253 (20) (1978) 7212–7215.
[44] H. Kohler, H. Jenzer, Interaction of lactoperoxidase with hydrogen peroxide: formation of enzyme intermediates and generation of free radicals, Free Radic. Biol. Med. 6 (3) (1989) 323–339, https://doi.org/10.1016/0891-5849(89)90059-2.
[45] J.M. Fukuto, S.J. Carrington, D.J. Tantillo, J.G. Harrison, L.J. Ignarro, B. A. Freeman, A. Chen, D.A. Wink, Small molecule signaling agents: the integrated chemistry and biochemistry of nitrogen oxides, oxides of carbon, dioxygen, hydrogen sulfide, and their derived species, Chem. Res. Toxicol. 25 (4) (2012) 769–793, https://doi.org/10.1021/tx2005234.
[46] J.A. Berzofsky, J. Peisach, B.L. Horecker, Sulfheme proteins. IV. The stoichiometry of sulfur incorporation and the isolation of sulfhemin, the prosthetic group of sulfmyoglobin, J. Biol. Chem. 247 (12) (1972) 3783–3791.
[47] M. Shieh, X. Ni, S. Xu, S.P. Lindahl, M. Yang, T. Matsunaga, R. Flaumenhaft, T. Akaike, M. Xian, Shining a light on SSP4: a comprehensive analysis and biological applications for the detection of sulfane sulfurs, Redox Biol. 56 (2022) 102433, https://doi.org/10.1016/j.redox.2022.102433.
[48] T. Akaike, T. Ida, F.-Y. Wei, M. Nishida, Y. Kumagai, M.M. Alam, H. Ihara, T. Sawa, T. Matsunaga, S. Kasamatsu, A. Nishimura, M. Morita, K. Tomizawa, A. Nishimura, S. Watanabe, K. Inaba, H. Shima, N. Tanuma, M. Jung, S. Fujii, Y. Watanabe, M. Ohmuraya, P. Nagy, M. Feelisch, J.M. Fukuto, H. Motohashi, Cysteinyl-tRNA synthetase governs cysteine polysulfidation and mitochondrial bioenergetics, Nat. Commun. 8 (1) (2017) 1177, https://doi.org/10.1038/s41467-017-01311-y.
[49] W. Jantschko, P.G. Furtmüller, M. Zederbauer, K. Neugschwandtner, C. Jakopitsch, C. Obinger, Reaction of ferrous lactoperoxidase with hydrogen peroxide and dioxygen: an anaerobic stopped-flow study, Arch. Biochem. Biophys. 434 (1) (2005) 51–59, https://doi.org/10.1016/j.abb.2004.10.014.
[50] I.I. Vlasova, Peroxidase Activity of Human Hemoproteins: Keeping the Fire under Control, vol. 23, 2018, p. 2561, 10.
[51] P. Nicholls, The formation and properties of sulphmyoglobin and sulphcatalase, Biochem. J. 81 (2) (1961) 374–383, https://doi.org/10.1042/bj0810374.
[52] J.A. Berzofsky, J. Peisach, W.E. Blumberg, I. Sulfheme Proteins, Optical and magnetic properties of sulfmyoglobin and its derivatives, J. Biol. Chem. 246 (10) (1971) 3367–3377, https://doi.org/10.1016/S0021-9258(18)62234-3.
[53] M.J. Chatfield, G.N. La Mar, 1H nuclear magnetic resonance study of the prosthetic group in sulfhemoglobin, Arch. Biochem. Biophys. 295 (2) (1992) 289–296, https://doi.org/10.1016/0003-9861(92)90520-7.
[54] L. Gharahbaghian, B. Massoudian, G. Dimassa, Methemoglobinemia and sulfhemoglobinemia in two pediatric patients after ingestion of hydroxylamine sulfate, West. J. Emerg. Med. 10 (3) (2009) 197–201.
[55] E. Román-Morales, E. López-Alfonzo, R. Pietri, J. López-Garriga, Sulfmyoglobin conformational change: a role in the decrease of oxy-myoglobin functionality, Biochem. Biophys. Reports 7 (2016) 386–393, https://doi.org/10.1016/j.bbrep.2016.07.002.
[56] R.P. Ferrari, E.M. Ghibaudi, S. Traversa, E. Laurenti, L. De Gioia, M. Salmona, Spectroscopic and binding studies on the interaction of inorganic anions with lactoperoxidase, J. Inorg. Biochem. 68 (1) (1997) 17–26, https://doi.org/10.1016/s0162-0134(97)00003-2.
[57] M.J. Chatfield, G.N. La Mar, K.M. Smith, H.K. Leung, R.K. Pandey, Identification of the altered pyrrole in the isomeric sulfmyoglobins: hyperfine shift patterns as indicators of ring saturation in ferric chlorins, Biochemist 27 (5) (1988) 1500–1507, https://doi.org/10.1021/bi00405a016.
[58] C.E. Cooper, G.C. Brown, The inhibition of mitochondrial cytochrome oxidase by the gases carbon monoxide, nitric oxide, hydrogen cyanide and hydrogen sulfide: chemical mechanism and physiological significance, J. Bioenerg. Biomembr. 40 (5) (2008) 533–539, https://doi.org/10.1007/s10863-008-9166-6.
[59] Y. Du, G. Liu, Y. Yan, D. Huang, W. Luo, M. Martinkova, P. Man, T. Shimizu, Conversion of a heme-based oxygen sensor to a heme oxygenase by hydrogen sulfide: effects of mutations in the heme distal side of a heme-based oxygen sensor phosphodiesterase (Ec DOS), Biometals 26 (5) (2013) 839–852, https://doi.org/10.1007/s10534-013-9640-4.
[60] M. Gajhede, D.J. Schuller, A. Henriksen, A.T. Smith, T.L. Poulos, Crystal structure of horseradish peroxidase C at 2.15 Å resolution, Nat. Struct. Biol. 4 (12) (1997) 1032–1038, https://doi.org/10.1038/nsb1297-1032.
[61] P.J. Mak, J.R. Kincaid, Resonance Raman spectroscopic studies of hydroperoxo derivatives of cobalt-substituted myoglobin, J. Inorg. Biochem. 102 (10) (2008) 1952–1957, https://doi.org/10.1016/j.jinorgbio.2008.07.005.
[62] A.D. Rodriguez-Mackenzie, L. Santos-Velazquez, H.D. Arbelo-Lopez, T. Wymore, J. Lopez-Garriga, Mechanistics of pH-dependent sulfmyoglobin formation: spin control and His64 proton relay, J. Chem. 2024 (2024) 4244579, https://doi.org/10.1155/2024/4244579.
[63] R. Pietri, A. Lewis, R.G. León, G. Casabona, L. Kiger, S.-R. Yeh, S. Fernandez-Alberti, M.C. Marden, C.L. Cadilla, J. López-Garriga, Factors controlling the reactivity of hydrogen sulfide with hemeproteins, Biochemist 48 (22) (2009) 4881–4894, https://doi.org/10.1021/bi801738j.
[64] E.A. Johnson, The reversion to haemoglobin of sulphhaemoglobin and its coordination derivatives, Biochim. Biophys. Acta 207 (1) (1970) 30–40, https://doi.org/10.1016/0005-2795(70)90134-0.
[65] A. Tomoda, A. Kakizuka, Y. Yoneyama, Oxidative and reductive reactions of sulphhaemoglobin with various reagents correlated with changes in quaternary structure of the protein, Biochem. J. 221 (3) (1984) 587–591, https://doi.org/10.1042/bj2210587.
[66] J. March, Advanced Organic Chemistry: Reactions, Mechanisms, and Structure, third ed., Wiley, 1985.
[67] E.I. Stiefel, Transition metal sulfur chemistry: biological and industrial significance and key trends, in: Transition Metal Sulfur Chemistry, American Chemical Society, 1996, pp. 2–38.
[68] E.S. Saltzman, W.J.C., Biogenic sulfur in the environment, ACS (Am. Chem. Soc.) Symp. Ser. (1987).
[69] T. Omori, Y. Saiki, K. Kasuga, T. Kodama, Desulfurization of alkyl and aromatic sulfides and sulfonates by dibenzothiophene-desulfurizing rhodococcus sp. strain SY1, Biosci. Biotechnol. Biochem. 59 (7) (1995) 1195–1198, https://doi.org/10.1271/bbb.59.1195.
[70] R. Javadli, A. de Klerk, Desulfurization of heavy oil, Appl. Petrochem. Res. 1 (1) (2012) 3–19, https://doi.org/10.1007/s13203-012-0006-6.
[71] P. Nagy, C.C. Winterbourn, Rapid reaction of hydrogen sulfide with the neutrophil oxidant hypochlorous acid to generate polysulfides, Chem. Res. Toxicol. 23 (10) (2010) 1541–1543, https://doi.org/10.1021/tx100266a.
[72] R. Greiner, Z. Pálinkás, K. Bäsell, D. Becher, H. Antelmann, P. Nagy, T.P. Dick, Polysulfides link H_2S to protein thiol oxidation, Antioxidants Redox Signal. 19 (15) (2013) 1749–1765, https://doi.org/10.1089/ars.2012.5041.
[73] C.H.K. Wu, The role of hydrogen sulphide in lung diseases, Biosci. Horiz.: Int. J. Stud. Res. 6 (2013) hzt009, https://doi.org/10.1093/biohorizons/hzt009.
[74] Q. Li, J.R. Lancaster, Chemical foundations of hydrogen sulfide biology, Nitric Oxide 35 (2013) 21–34, https://doi.org/10.1016/j.niox.2013.07.001.